31st Annual International Conference of the IEEE EMBS
Minneapolis, Minnesota, USA, September 2-6, 2009

Deep Brain Stimulation that Abolishes Parkinsonian Activity in Basal Ganglia Improves Thalamic Relay Fidelity in a Computational Circuit

Alan D. Dorval, Neil Panjwani, Rosa Y. Qi, and Warren M. Grill, *Sr. Member, IEEE*

Abstract – **Deep brain stimulation (DBS) of the subthalamic nucleus reduces the severity of parkinsonian motor symptoms, but the therapeutic mechanisms are not understood. We hypothesize that clinically effective high frequency DBS suppresses disordered neuronal activity in the globus pallidus internus (GPi), a primary output structure of the basal ganglia. In a computational model of the basal ganglia thalamic circuit, periodic high frequency (>100Hz) stimulation of the subthalamic nucleus reduced the incidence of thalamic cell errors, from the high error rates seen in the parkinsonian case back to the low error rates seen in the normal-healthy case. In contrast, both low frequency (<70Hz) DBS and high frequency aperiodic DBS failed to alleviate thalamic errors. In high error rate conditions, disordered patterns of GPi activity lead to irregular synaptic inhibition of thalamus. In low error rate conditions, ordered patterns of GPi activity lead to regular synaptic inhibition of thalamus. Linear regression revealed that the variance of the GPi synaptic output accounted for 87-97% of the changes in thalamic error rate. In contrast, the average GPi synaptic output – a measure of total GPi activity – accounted for only 25-50% of the changes in thalamic error rate. Thus, while the firing rate of GPi cells may play some minor role, regularizing the pathological patterns of GPi activity is the mechanism by which DBS treats parkinsonian motor symptoms.**

I. Introduction

Deep brain stimulation (DBS) of some basal ganglia regions can reduce tremor and hypokinetic symptoms in persons whose Parkinson's disease has become medically refractory. For DBS to be effective, the frequency of stimulation must exceed ~100 Hz. Furthermore, all clinically used DBS patterns are perfectly regular. For example, if DBS is presented at 100 Hz then consecutive DBS pulses are always and exactly 10 msec apart.

Despite broad and growing application, the mechanisms by which DBS attains symptom relief are not fully understood. Recent studies suggest that DBS increases the firing rate of fibers projecting from the site of stimulation [1][2][3][4]. In addition to firing rate changes however, parkinsonian symptoms may correlate with spike time variability or unique patterns of neuronal activity [5][6][7][8][9]. High frequency DBS may minimize parkinsonian motor symptoms by suppressing the pathological patterns of neuronal activity present in the parkinsonian basal ganglia.

To test the extent of DBS-induced pathological activity suppression, a computational model of the basal ganglia thalamic circuit was implemented with minor modifications from previously published versions [10][11]. Parameter changes shifted the model between the normal-healthy and parkinsonian conditions. In the parkinsonian case, different patterns of DBS were presented to the subthalamic nucleus. Model thalamic neurons were tasked with converting an input pulse train into an output spike train. The thalamic error rate – the average number of mistakes made by one thalamic neuron in one second – was calculated as a surrogate for symptom severity.

The parkinsonian version of the model was presented with DBS patterns at a range of frequencies (7 to 150 Hz) and variabilities (0 to 60%). We hypothesized that DBS patterns would reduce (or not reduce) the thalamic error rate if they managed to regularize (or not regularize) output from the basal ganglia. In this study, the normal-healthy condition and the parkinsonian in response to high frequency periodic DBS conditions yielded highly regular basal ganglia output and low thalamic error rates. In contrast, the parkinsonian version of the model in response to either low frequency DBS or high frequency aperiodic DBS yielded highly irregular basal ganglia output and high thalamic error rates. Thus, clinically effective DBS improves thalamic relay fidelity by regularizing basal ganglia output.

II. Computational Methods

Computational implementations, experiments and analyses were performed on computers running various distributions of the GNU/Linux operating system (Free Software Foundation, Boston MA). All models and analysis code are available from the authors upon request.

A. Circuit Model Implementation

The computational model was modified from an existing model of the basal ganglia thalamic network [10][11]. Briefly, the model was composed of 8 or 16 point neurons in each of the basal ganglia regions (subthalamic nucleus, STN; globus pallidus externus, GPe; globus pallidus internus, GPi) and in the pallidal receiving thalamus, TC. In the 3 basal ganglia regions, neuronal membrane potential (V) was set: $c_m\, dV/dt = I_{app} - I_{Na} - I_K - I_{Ca} - I_T - I_{ahp} - I_L - I_{syn}$, where c_m is the membrane capacitance and each I variable represents a

Manuscript received April 7, 2009. This work was supported in part by the U.S. National Institutes of Health under grants K25-NS053544 (ADD) and R01-NS040894 (WMG).

A.D. Dorval was with the Department of Biomedical Engineering, Pratt School of Engineering, Duke University, Durham, NC 27708 USA. He is now with the Department of Bioengineering, University of Utah, Salt Lake City, UT 84112 USA (phone: 919-660-5250; fax: 919-684-4488; email: alan.dorval@utah.edu).

N. Panjwani is with the Department of Biomedical Engineering, Pratt School of Engineering, Duke University, Durham, NC 27708 USA (email: neil.panjwani@duke.edu).

R. Y. Qi is with the Department of Biomedical Engineering, Pratt School of Engineering, Duke University, Durham, NC 27708 USA (email: rosa.qi@duke.edu).

W. M. Grill is with the Department of Biomedical Engineering, Pratt School of Engineering, Duke University, Durham, NC 27708 USA (email: warren.grill@duke.edu).

current source. Thalamic membrane potential was described as: $c_m\, dV/dt = I_{app} - I_{Na} - I_K - I_T - I_L - I_{syn}$. The ionic currents ($I_{Na}\ I_K\ I_{Ca}\ I_T\ I_{ahp}\ I_L$), their gating variables and the parameters for the synaptic connections described below have been published elsewhere (e.g., [11]).

Applied Currents, I_{app}. The GPe and GPi neurons were biased with applied currents that varied between the normal-healthy and parkinsonian conditions, modeling changes in the strength of striatal inhibition. Neurons in GPi received 21 and 12 pA/μm^2 depolarizing current in the normal-healthy and parkinsonian conditions, respectively. Neurons in GPe received an average of 20 and 5 pA/μm^2 depolarizing current in the normal-healthy and parkinsonian conditions, respectively. To provide network heterogeneity however, one-fourth of GPe cells received 2 pA/μm^2 above the mean, and another one-fourth received 2 pA/μm^2 below the mean. The STN neurons received 25 pA/μm^2 depolarizing current, plus 300 pA/μm^2 excitation coincident with each DBS pulse and lasting for 300 μsec. The TC cells included no bias current, but did receive depolarizing pulses of 2 pA/μm^2 lasting 5 msec, which modeled sensory-motor input. Each instantaneous frequency (i.e., the reciprocal of inter-pulse interval) was drawn from a gamma distribution with a mean of 10 Hz and a standard deviation of 2 Hz.

Synaptic Connections, I_{syn}. The neurons were connected in a sparse, structured fashion as follows: each STN neuron received input from 2 GPe neurons (GPe^{k+1}&$GPe^k \rightarrow STN^k$); each GPe neuron received input from 2 neighbors and 2 STN neurons (GPe^{k+2},GPe^{k+1},STN^k&$STN^{k-1} \rightarrow GPe^k$); each GPi neuron received input from 2 GPe and 2 STN neurons (GPe^{k+2},GPe^{k+1},STN^k&$STN^{k-1} \rightarrow GPi^k$); and each TC neuron received input from 2 GPi neurons (GPi^{k+1}&$GPi^k \rightarrow TC^k$). For the varying DBS frequency simulations only (Fig. 1), the STN efferent synapses were described by an alpha function $\{z(t) = t\ exp(-t/\tau_{syn}),\ t>0\}$ convolved with the STN spike times. All other synaptic connections were described by a differential equation $dz/dt = \alpha(1 - z)z_\infty - \beta z$, where $z_\infty = [1 + exp((V - \theta_z)/\sigma_z)]^{-1}$. From each synaptic gating variable z, the current was found as: $I_{syn} = G_{syn}\, z\, (V - V_{syn})$.

B. Network Simulations

Two sets of computational experiments were performed: DBS-frequency and DBS-variability. The DBS-frequency set was simulated in the numerical computing environment, Matlab (The Mathworks Inc., Natick MA), and the DBS-variability set was run in the differential equation package XPP-AUT (http://www.math.pitt.edu/~bard/xpp/xpp.html). Simulations were run with the fourth order Runge-Kutta solver using a maximum time step of 10 or 50 μsec, with 8 or 16 neurons per region, in the DBS-frequency or DBS-variability sets, respectively. The only other model difference was the STN efferent synapse, described above.

The DBS-frequency set included a normal-healthy case, a parkinsonian case without DBS, and four parkinsonian cases with DBS at varying frequencies: 150 Hz, 70 Hz, 20 Hz and 7 Hz. Summary data were calculated from 300 sec of simulation time. The DBS-variability set included a normal-healthy case, a parkinsonian case without DBS, and four parkinsonian cases with 130 Hz DBS at different levels of variability: 0%, 10%, 30% and 60%. The variability measures quantify the standard deviation of the instantaneous frequency as a percentage of the mean. Each instantaneous frequency (i.e., the reciprocal of inter-pulse interval) was drawn from a gamma distribution with a mean of 130 Hz and standard deviations of 0, 13, 39 or 78 Hz for the 0%, 10%, 30% or 60% cases, respectively. Summary data were calculated from 150 sec of simulation time.

III. Analysis & Results

A. Responses to DBS of Different Frequencies

A computational model of the basal ganglia thalamic circuit was simulated under normal-healthy, parkinsonian, and parkinsonian with DBS conditions. Four different frequencies were applied to the subthalamic nucleus (STN) for the parkinsonian with DBS conditions. Thalamic (TC) neurons received the same train of excitatory input pulses in all conditions. Thalamic responses were characterized as correct if the TC cell spiked once within a 25 msec window following the input pulse, and incorrect if the TC cell spiked more than once or not at all. An error rate was calculated as the average number of incorrect responses per second across all TC neurons in each condition (Fig. 1a). Errors were rare in the normal-healthy case, but became common in the parkinsonian case. High frequency DBS greatly reduced the error rate from the parkinsonian level, but low frequency DBS did not.

The logarithms of inter-spike intervals (ISIs) of all GPi cells were tabulated and converted into probability densities for each condition [12]. Probability densities from the asymptomatic conditions (Fig. 1b, left) were both narrower and more peaked, with higher peak probabilities, than densities from the symptomatic conditions (Fig. 1b, right). In particular, the symptomatic cases included many long ISIs (>25 msec) that were nearly absent in the asymptomatic cases. The ISI entropy was calculated to quantify the changes in ISI distributions: $H = -\Sigma\, P_k\, log_2\, P_k$, where the ISI probability densities were converted into probability distributions with 50 ISI bins per decade, the sum was taken over all ISI bins and P_k is the probability associated with the k^{th} bin. Note the similarities between the GPi cell entropy (Fig. 1c) and the thalamic error rate.

B. Responses to DBS of Different Variabilities

A computational model of the basal ganglia thalamic circuit was simulated under normal-healthy, parkinsonian, and parkinsonian with DBS conditions. High frequency DBS (130 Hz) patterns with 4 degrees of variability – 0%, 10%, 30% and 60% – were applied to STN for the parkinsonian with DBS conditions. Thalamic neurons received the same train of excitatory input pulses in all conditions. Error rates were calculated as described above. Errors were rare in the normal-healthy case, but became common in the parkinsonian case (Fig. 2a). Highly regular (periodic) DBS greatly reduced the error rate from the parkinsonian level, but irregular (aperiodic) DBS did not.

The probability densities of the logarithms of the GPi cell ISIs were found for each condition. Probability densities from the asymptomatic conditions (Fig. 2b, left) were both narrower and more peaked, with higher peak probabilities, than densities from the symptomatic conditions (Fig. 2b, right). In particular, the symptomatic cases included many

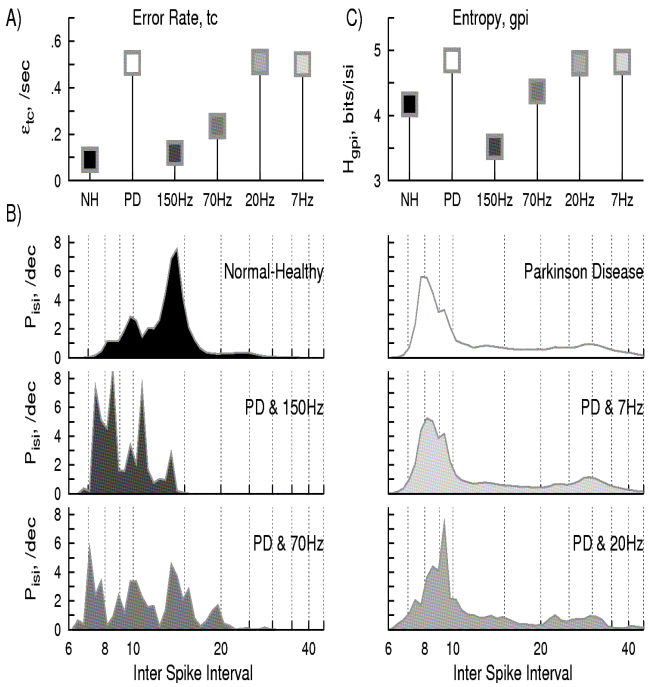

Fig. 1. Effects of DBS Frequency. A) Thalamic error rates as a function of condition: normal-healthy (NH), parkinson disease (PD), and PD with DBS at 150, 70, 20 and 7 Hz. B) Probability densities of the logarithm of GPi ISIs in the identified cases. C) Entropies of the GPi ISIs, calculated from the probability densities, parallel the error rates.

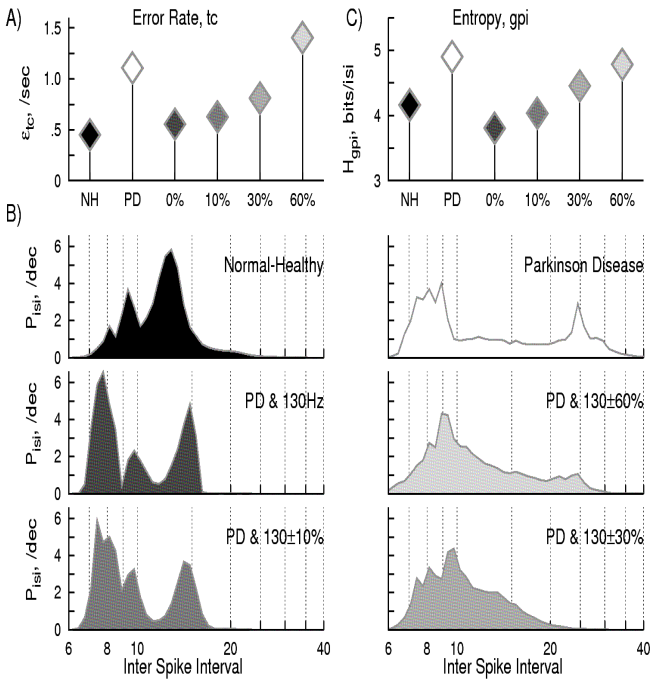

Fig. 2. Effects of DBS Variability. A) Thalamic error rates as a function of condition: NH, PD, and PD with 130 Hz DBS with 0%, 10%, 30% and 60% variability. B) Probability densities of the logarithm of GPi ISIs in the identified cases. C) Entropies of the GPi ISIs, calculated from the probability densities, parallel the error rates.

long ISIs (>25 msec) that were nearly absent in the asymptomatic cases. The ISI entropy (Fig. 2c) paralleled the thalamic error rates.

C. Synaptic Variability

To examine the effects that the inhibitory GPi efferents had on thalamic errors in all conditions, the synaptic conductances were analyzed. The means and standard deviations of the GPi synaptic conductances inhibiting the TC neurons were found for the DBS-frequency and DBS-variability sets (Fig. 3a). While the mean conductances varied only minimally between conditions, the standard deviation of the conductances varied greatly, tracking the changes in thalamic error rates.

A best linear fit was made to the conductance means and standard deviations as a function of the thalamic error rate (Fig. 3b). The mean conductance (tracking the GPi firing rate) could only account for 25% of the error rate variance in the DBS-variability set. Furthermore, while frequency appeared to account for 50% of the thalamic error rate variance in the DBS-frequency set, the two outliers that constitute nearly all of the remaining variability are the normal-healthy and parkinsonian with the clinically used 150Hz DBS cases (Fig 3b, top-left). Thus, the regression analysis fails most notably on two of the three data points that happen to be clinically relevant. In contrast, synaptic variance accounted for 87-97% of thalamic error rate.

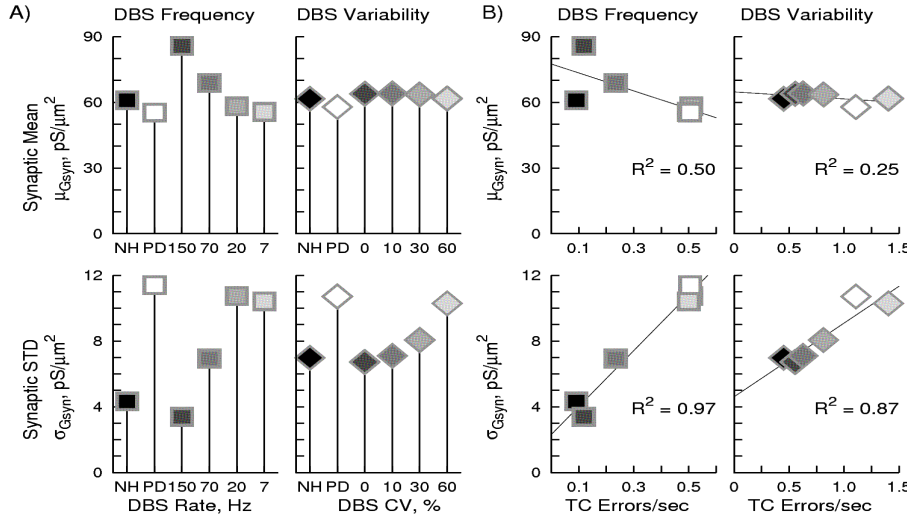

Fig. 3. GPi Output Synaptic Statistics. Inhibitory conductance means (top) and standard deviations (bottom) for the DBS-frequency (left, squares) and DBS-variability (right, diamonds) sets as a function of condition (A) and thalamic error rates (B). Best fit linear regressions show that the standard deviation of the conductance is highly correlated with the thalamic error rate.

IV. Discussion

Deep brain stimulation (DBS) of the subthalamic nucleus (STN) has become a common therapy to treat the motor symptoms of parkinsonism, but the mechanisms remain elusive. Symptoms may follow from pathological neuronal activity in the basal ganglia [13][14][15]. We used a computational model of the relevant neural structures to test the hypothesis that clinically used DBS alleviates motor symptoms by regularizing the pathological synaptic activity of the basal ganglia output structure, the globus pallidus internus (GPi). Using thalamic error rate as a surrogate for symptom severity, we showed that both low frequency DBS and high frequency aperiodic DBS did not regularize GPi synaptic activity, and did not improve thalamic error rate. In contrast, periodic high frequency DBS did regularize GPi activity and did improve thalamic error rates.

These results are supported by experimental results which found that GPi firing rates changes in the parkinsonian condition and in response to DBS were small in comparison with changes in regularity and bursting activity [3][5][6][7][9][13][16]. In a related study, model thalamic neurons experienced decreased or increased fidelity in response to parkinsonian firing patterns or DBS-induced firing patterns, respectively [17].

The present results demonstrate that low frequency DBS and high frequency aperiodic DBS both fail to alleviate symptoms in the same way: they do not improve thalamic error rates because they do not regularize GPi neuronal activity. Thus, the periodicity of clinically used DBS is crucial for its success. Furthermore, low frequency DBS fails because it drives the GPi cells to slowly to force regular activity. Indeed, all conditions that had no GPi ISIs over ~25 msec had much lower entropies and error rates (Figs. 1 & 2). Thus, while the average firing rate may be of little importance, keeping the longest GPi ISIs below some maximum may be secret to DBS effectiveness.

Finally, while some motor symptoms of parkinsonism are well treated by periodic high frequency DBS in some persons, the therapy does not work for all individuals and other symptoms persist. The ideal DBS may be one that, rather than forcing regular GPi activity, restores GPi activity to the healthy condition (e.g., Figs 1b & 2b, top-left). We will continue to search for these optimal DBS patterns.

Acknowledgment

We thank A. Wongsarnpigoon for help establishing the DBS-frequency simulations.

References

[1] Windels F, Bruet N, Poupard A, Bertrand A, Feuerstein C, Savasta M, "Influence of the frequency parameter on extracellular glutamate and gamma-aminobutyric acid in substantia nigra and globus pallidus during electrical stimulation of subthalamic nucleus in rats," *J Neurosci Res*, vol. 72, pp. 259-267, April 2003.

[2] Anderson ME, Postupna N, Ruffo M, "Effects of high-frequency stimulation in the internal globus pallidus on the activity of thalamic neurons in the awake monkey," *J Neurophysiol*, vol. 89, pp. 1150-1160, February 2003.

[3] Hashimoto T, Elder CM, Okun MS, Patrick SK, Vitek JL, "Stimulation of the subthalamic nucleus changes firing pattern of pallidal neurons," *J Neurosci*, vol. 23, pp. 1916-1923, March 2003.

[4] McIntyre CC, Grill WM, Sherman DL, Thakor NV, "Cellular effects of deep brain stimulation: model-based analysis of activation and inhibition," *J Neurophysiol*, vol. 91, pp. 1457-1469, April 2004.

[5] Wichmann T, DeLong MR, "Pathophysiology of Parkinson's disease: the MPTP primate model of the human disorder," *Ann NY Acad Sci*, vol. 991, pp. 199-213, June 2003.

[6] Bar-Gad I, Elias S, Vaadia E, Bergman H, "Complex locking rather than complete cessation of neuronal activity in the globus pallidus of a 1-methyl-4-phenyl-1,2,3,6-tetrahydropyridine-treated primate in response to pallidal microstimulation," *J Neurosci*, vol. 24, pp. 9410-9419, August 2004.

[7] Meissner W, Leblois A, Hansel D, Bioulac B, Gross CE, Benazzouz A, Boraud T, "Subthalamic high frequency stimulation resets subthalamic firing and reduces abnormal oscillations," *Brain*, vol. 128, pp. 2372-2382, August 2005.

[8] Asanuma K, Tang C, Ma Y, Dhawan V, Mattis P, Edwards C, Kaplitt MG, Feigin A, Eidelberg D, "Network modulation in the treatment of Parkinson's disease," *Brain*, vol. 129, pp. 2667-2678, July 2006.

[9] Dorval AD, Russo GS, Hashimoto T, Xu W, Grill WM, Vitek JL, "Deep brain stimulation reduces neuronal entropy in the MPTP-primate model of Parkinson's disease," *J Neurophysiol*, vol. 100, pp. 2807-2818, November 2008.

[10] Terman D, Rubin J, Yew AC, Wilson CJ, "Activity patterns in a model for the subthalamopallidal network of the basal ganglia," *J Neurosci*, vol. 22, pp. 2963-2976, April 2002.

[11] Rubin JE, Terman D, "High frequency stimulation of the subthalamic nucleus eliminates pathological thalamic rhythmicity in a computational model," *J Comput Neurosci*, vol. 16, pp. 211-235, May-June 2004.

[12] Dorval AD, "Probability distributions of the logarithm of inter-spike intervals yield accurate entropy estimates from small datasets," *J Neurosci Methods*, vol. 173, pp. 129-139, August 2008.

[13] Bergman H, Wichmann T, Karmon B, DeLong MR, "The primate subthalamic nucleus. II. Neuronal activity in the MPTP model of parkinsonism," *J Neurophysiol*, vol. 72, pp. 507-520, August 1994.

[14] Magnin M, Morel A, Jeanmonod D, "Single-unit analysis of the pallidum, thalamus and subthalamic nucleus in parkinsonian patients," *Neurosci*, vol. 96, pp. 549-564, January 2000.

[15] Wichmann T, Soares J, "Neuronal firing before and after burst discharges in the monkey basal ganglia is predictably patterned in the normal state and altered in parkinsonism," *J Neurophysiol*, vol. 95, pp. 2120-2133, December 2006.

[16] Soares J, Kliem MA, Betarbet R, Greenamyre JT, Yamamoto B, Wichmann T, "Role of external pallidal segment in primate parkinsonism: comparison of the effects of 1-methyl-4-phenyl-1,2,3,6-tetrahydropyridine-induced parkinsonism and lesions of the external pallidal segment," *J Neurosci*, vol. 24, pp. 6417-6426, July 2004.

[17] Guo Y, Rubin JE, McIntyre CC, Vitek JL, Terman D, "Thalamocortical relay fidelity varies across subthalamic nucleus deep brain stimulation protocols in a data-driven computational model," *J Neurophysiol*, vol. 99, pp. 1477-1492, January 2008.